https://rbgeomorfologia.org.br/
ISSN 2236-5664

Revista Brasileira de Geomorfologia

v. 27, nº1 (2026)

http://dx.doi.org/10.20502/rbg.v27i1.2741

Artigo de Pesquisa

Ice Phenology of Lakes in the Byers, Keller, and Fildes Peninsulas, Maritime Antarctica, from 2014 to 2023 using SAR Data

Fenologia do gelo de lagos nas penínsulas Byers, Keller e Fildes, Antártica Marítima, no período de 2014 – 2023 com dados SAR

Jorge Antônio Viel [1], Kátia Kellem da Rosa [2], Carina Petsch [3], Luiz Felipe Velho [4], Danielle Dall Amaria Soffiatti [5], Federico Aita [6] and Rosemary Vieira [7]

[1] Federal Institute of Education, Science and Technology of Rio Grande do Sul, *Campus* Bento Gonçalves, Bento Gonçalves, Brazil. ja-viel89@hotmail.com
ORCID: https://orcid.org/0000-0002-4139-9623

[2] Federal University of Rio Grande do Sul, Geography Department, Porto Alegre, Brazil. katiakellem@gmail.com
ORCID: https://orcid.org/0000-0003-0977-9658

[3] Federal University of Santa Maria, Geosciences Department, Santa Maria, Brazil. carinapetsch@gmail.com
ORCID: https://orcid.org/0000-0002-1079-0080

[4] Federal Institute of Education, Science and Technology of Rio Grande do Sul, *Campus* Porto Alegre, Porto Alegre, Brazil. lfvelho@gmail.com
ORCID: https://orcid.org/0000-0001-9543-7544

[5] Federal University of Rio Grande do Sul, Geography Department, Porto Alegre, Brazil. danielled.soffiatti@gmail.com
ORCID: https://orcid.org/0009-0003-0381-9775

[6] Federal University of Rio Grande do Sul, Geography Department, Porto Alegre, Brazil. federico.aita2704@gmail.com
ORCID: https://orcid.org/0009-0007-5447-8498

[7] Fluminense Federal University, Geography Department, Niterói, Brazil. rosemaryvieira@id.uff.br
ORCID: https://orcid.org/0000-0003-0312-2890

Received: 18/08/2025; Accepted: 23/01/2026; Published: 27/03/2026

Abstract: This study examined the ice phenology of twenty-five lakes located in the Fildes and Keller peninsulas (King George Island) and the Byers Peninsula Livingston Island), Antarctica, using SAR (Sentinel-1) data from 2014 to 2023. A backscatter threshold was established for ice-free and frozen surfaces in S1 images. The temporal analysis of lake phenology was conducted covering the months from October to March. The slope context, altitude, and distance from the coast of the lakes were characterized. Field activities were carried out to validation. Temporal backscatter analysis revealed seasonal patterns of lake surface freezing and thawing, which were correlated with climatic variables, including mean air temperature, precipitation, and wind. Mean air temperature emerged as the primary driver of ice cover variability, with fewer frozen days observed in years of increased positive temperatures, particularly during El Niño events. The years 2015 and 2019 exhibited less thawing, while 2023 recorded the lowest extent of frozen lake surfaces (99.15%). Local factors, including wind speed and direction, and coast distance and altitude, also influenced the observed patterns. Sentinel-1 imagery proved effective for mapping and monitoring lake surface ice cover in glacial and periglacial environments, underscoring its potential for assessing lacustrine responses to climate variability.

Keywords: Proglacial lakes 1; seasonal behavior 2; snow and ice cover 3; climate change 4; SAR 5.

Resumo: Esta pesquisa investigou a fenologia do gelo em vinte e cinco lagos das penínsulas Fildes e Keller (Ilha Rei George) e Byers (Ilha Livingston), Antártica, utilizando dados SAR (Sentinel-1), entre 2014 e 2023. Foi aplicado um limiar de retroespalhamento para a superfície congelada nas imagens. A fenologia dos lagos foi analisada para os meses de outubro a

março. Os lagos foram caracterizados quanto ao contexto de declividade, altitude e distância da costa. Atividades de campo foram realizadas para a validação. As variações do retroespalhamento e do congelamento e descongelamento da superfície dos lagos estão relacionadas com a temperatura média do ar, precipitação e vento. A temperatura média do ar é o principal fator na variação da cobertura de gelo, com redução no número de dias congelados em anos com maior ocorrência de temperaturas positivas, especialmente durante eventos *El Niño*. 2015 e 2019 apresentaram menor descongelamento e 2023 apresentou a menor extensão da ocorrência (99,15%) da superfície com gelo. Variações de velocidade e direção do vento, além do contexto geográfico dos lagos, como a distância da costa e a altitude, influenciaram as diferenças entre os lagos. As imagens SAR demonstraram eficácia para o mapeamento e monitoramento da cobertura de gelo superficial em ambientes glaciais e periglaciais, evidenciando seu potencial em estudos de resposta lacustre à variabilidade climática.

Palavras-chave: Lagos proglaciais 1; comportamento sazonal 2; cobertura de neve e gelo 3; mudanças climáticas 4; SAR 5.

1. Introduction

The South Shetland archipelago is located in the Maritime Antarctic region. This region is important for environmental monitoring because Antarctic and sub-Antarctic glaciers at latitudes near 60° S, and with lower continentality, are more sensitive in their mass balance than glaciers at higher latitudes — a factor explained by greater maritime influence and temperatures closer to the pressure-melting point (MARSHALL, 2021). In addition, subpolar glaciers and landscapes are prone to undergo transformations on decadal timescales in response to global warming (MARSHALL, 2021). For example, recent climate change has impacted natural systems, including changes in the spatial distribution of glacial systems (CARRIVICK & HECKMANN, 2017). Consequently, glacier-covered areas are replaced by ice-free areas where rapid formation and an increase in the number of lakes occur (SHUGAR et al., 2020).

In this context, the Antarctic Peninsula (AP) region has experienced one of the fastest atmospheric warmings on the planet since the 1950s (VAUGHAN et al., 2003; TURNER, 2004; JONES et al., 2016; BLITZ et al., 2018; TURNER et al., 2021). In the AP region over recent decades there has also been a significant increase in ice-free areas (SHUGAR et al., 2020), the emergence of new lakes and an increase in their surface areas, as demonstrated by Petsch et al. (2022). Monitoring the behavior of lake surface melt is therefore relevant within the context of improving our understanding of climate change impacts in this region of the planet.

Glacial lakes and their components are recognized as important indicators of cryosphere behavior (CARRIVICK & HECKMANN, 2017). The periodic formation of lakes and the reduction of ice cover over time — as a result of seasonal and interannual climate variations — are referred to as lake ice phenology (KROPÁČEK et al., 2013; ŠMEJKALOVÁ et al., 2016).

Accordingly, the freeze and thaw behavior of ice in glacial lakes can indicate air temperature variations across different timescales (ZHANG & PAVELSKY, 2019). Lake ice cover is essential to limit winter evaporation rates; without it, lake levels, the extent of surface waters and ultimately the available freshwater would be drastically reduced (WOOLWAY et al., 2020). However, there is limited understanding of the spatial patterns of phenology or how these patterns are influenced by various climatic and geomorphological factors (O'REILLY et al., 2015), particularly for Antarctica, including its subpolar maritime region.

Surface melt and freeze of lakes on Fildes Peninsula in the Maritime Antarctic were analyzed by Rosa et al. (2020) for the period July 2016 to December 2018, demonstrating the potential of Sentinel-1A (S1). In this vein, satellite remote sensing provides a viable alternative to detect and monitor changes in lake ice cover at high latitudes (DUGUAY et al., 2012; ZHANG & PAVELSKY, 2019). Synthetic Aperture Radar (SAR) images have been used to characterize lake ice phenology in polar regions (PETSCH et al., 2020; DIRSCHERL et al., 2021). Assessing the potential and limitations of SAR imagery, such as S1, is relevant to establish a monitoring network for variability in lake ice cover in ice-free areas. Thus, the objective of the present work is to investigate the ice henology of twenty-five lakes located in ice-free areas of the Fildes, Byers and Keller peninsulas, Antarctica, and their response to climatic variability through temporal analysis of SAR images for the period 2014–2023.

2. Study Area

The study evaluates the phenology of lakes located on three distinct peninsulas of the South Shetland Islands, situated in the Maritime Antarctic (Figure 1). There are numerous lakes in the ice-free areas of the South Shetland Islands; the largest of these are located on Byers Peninsula (Livingston Island) and Fildes Peninsula (King George Island). Therefore, these lakes occur within a unique geographic context, with specific glacial and periglacial conditions, as demonstrated by Petsch et al. (2022). Most research on lakes in the ice-free areas of the South Shetland Islands focuses on mineralogical, chemical and geochemical characterization of lake sediments (ALFONSO et al., 2015; VIEIRA et al., 2015; GALVÃO et al., 2020), and there is no historical record of these lakes' phenology. For the Antarctic subpolar region, information, and monitoring of lake ice phenology are still incipient. Moreover, there is not a significant number of investigations into the influence of characteristics such as area and geographic context on the behavior of lakes' surface ice cover. On the Keller, Byers and Fildes peninsulas there are lakes that supply Antarctic stations and that could benefit in their logistical planning from information on lake surface ice phenology. Thus, 13 lakes located on Fildes Peninsula, 10 lakes on Byers Peninsula and 2 lakes on Keller Peninsula were studied (Chart 1).

The Fildes and Keller peninsulas are located on King George Island (KGI), which is the largest island of the South Shetland Islands, with approximately 1,250 km². Livingston Island (LI), where Byers Peninsula is located, is the second-largest island of the archipelago. Both islands are delimited to the north by the Drake Passage and to the south by the Bransfield Strait.

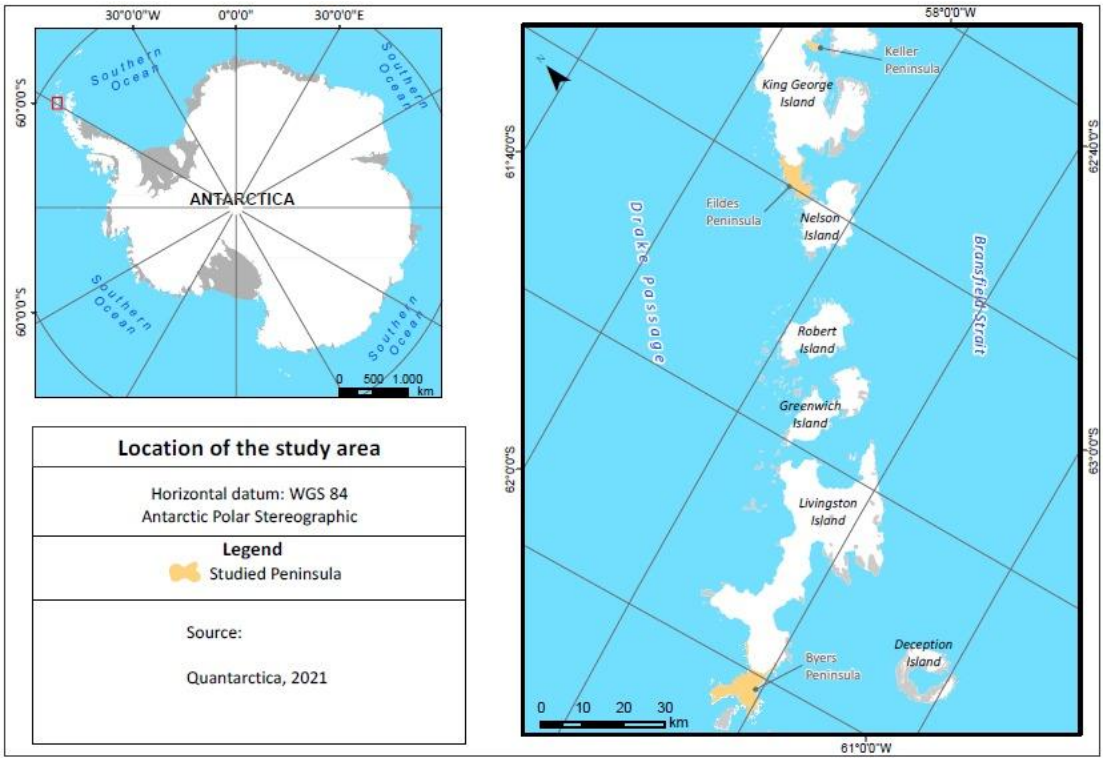

Figure 1. Location of the study area. Source: *Quantarctica* (MATSUOKA *et al*., 2018).

Fildes Peninsula is bounded to the northeast by Collins Glacier, covers 15 km², is located in the western sector of KGI (Maxwell Bay) and has a maximum elevation of 270 m. Its relief is predominantly characterized by eroded surfaces, flat surfaces on marine terraces and elevated interior surfaces (CURL, 1980), forming a set of platforms with gently undulating relief (ANDRADE, 2017). Glacial-fluvial channels, common in ice-free areas of the Maritime Antarctic during summer, have a high capacity to shape periglacial geomorphology, resulting in V-shaped valley forms (ANDRADE, 2017).

Keller Peninsula, where the Brazilian Comandante Ferraz Antarctic Station (EACF) is located, lies in Admiralty Bay and has a maximum elevation of 332.8 m (Mount Birkenmajer). Keller Peninsula's relief is predominantly classified as strongly undulating and mountainous (MENDES JR et al., 2010). These two classes

occupy nearly 50% of Keller Peninsula. Its relief is characterized by variably sized detrital accumulations and diverse features such as terrace levels and moraines, talus deposits and rocky ridges (FRANCELINO et al., 2004).

Byers Peninsula has the largest extent of ice-free area in the Maritime Antarctic (FARIA, 2010). It is located in the western sector of Livingston Island; it covers 60 km² and has a maximum elevation of 150 m. It is bounded to the northeast by Ivanov Beach, separated by Rotch Dome and the Urvich Ridge to the east. The deglaciated area of Byers Peninsula is characterized by numerous glacier-eroded valleys, frequently forming lakes, including Limnopolar (PABLO, 2024). Furthermore, its lithological composition and geological structure partly condition the peninsula's topography, with main relief features located in volcanic rock sectors where prominent hills and small promontories coincide with basaltic or andesitic outcrops (FARIA, 2010). Finally, various channels and lakes are identified, the largest being Midge, Limnolar and Basalt (IVANOV, 2010).

Chart 1. Area and codes of the lakes studied on the Fildes, Keller and Byers Peninsulas. UTM coordinates, WGS 84 horizontal datum, Zone 21, (Fildes and Keller peninsulas) and Zone 20 (Byers peninsula).

Location	Code	Lake area (ha)	Geometric altitude (m)	Lake coordinate central point (UTM)	
				East (m)	North (m)
Fildes Peninsula	1	9,57	29	400528	3103711
	2	9,32	38	397678	3102696
	3	4,14	36	398476	3101437
	4	3,71	69	397699	3101437
	5	3,07	63	398940	3105321
	6	3,00	88	398738	3105052
	7	2,72	42	397580	3103226
	8	2,58	108	400569	3104268
	9	1,95	141	396123	3099200
	10	1,39	63	397806	3100071
	11	1,17	84	398648	3106056
	12	1,15	144	395833	3099233
	13	1,11	83	399746	3105525
Keller	14	0,22	9	427204	3115465

Peninsula	15	0,18	5	427233	3115723
Byers Peninsula	1	4,48	75	597695	6945836
	2	3,63	0	594728	6949365
	3	3,48	0	595101	6947905
	4	3,14	71	597494	6946479
	5	2,58	0	594866	6950069
	6	2,56	0	595729	6946520
	7	2,44	68	598221	6945389
	8	1,61	49	603842	6947828
	9	1,37	51	604007	6947680
	10	1,31	57	597111	6947815

3. Materials and Methods

3.1. Data

To compile the research database, various materials from different sources were used (Chart 2). Note that the SAR data were processed using the Sentinel Application Platform (SNAP) and that ArcGIS was used for integrating spatial data — both vector and raster.

Chart 2. Data produced and used in the research.

Data	Acquisition mode and polarization	Period	Data structure	Spatial resolution (m)	Relative vertical accuracy (m)	Source
Sentinel-1A C banda SAR sensor	IW (HH+HV)	2014-2023	Raster	10	-	ESA
DEM REMA 8	-	2018	Raster	8,8	0,6	PGC
Lakes edge	-	2023	Vector	-	-	Petsch et al. (2018)
Lakes edge by NDWI	-	2023	Vector	-	-	Petsch et al. (2022)

Sentinel-1A (S1) images in IW mode are provided every 12 days and were acquired for the period 2014 –2023. The images are Level-1 GRD (Ground Range Detected) products and use the C-band to acquire data (ESA, 2022). The incidence angle ranges from 29.1° to 46°. The images were obtained free of charge from the European Space

Agency (ESA) website. Sentinel images in IW mode were chosen because they are freely available; moreover, being SAR data, they can be used regardless of cloud cover. For terrain correction during image processing, the REMA 8 digital elevation model (Reference Elevation Model of Antarctica) with an 8-meter spatial resolution was used.

Two complementary techniques were used to delineate lake perimeters on Keller and Fildes peninsulas. First, lakes were vectorized using a Sentinel-1A radar image dated 25 February 2020. This date was chosen because, according to the Copernicus Climate Change Service (C3S), February 2020 recorded atypically high air temperatures for the region; therefore the likelihood of the studied lakes having frozen surface areas was practically nil. The image was classified according to a backscatter threshold, with values below −15 dB considered to indicate ice-free water (VIEL et al., 2022).

Similarly, the lake boundaries published in Petsch et al. (2022) were used. Those authors used a Landsat 8 OLI image with 30-meter spatial resolution and applied the NDWI index to inventory and map lakes in the study area. This approach was used for the initial lake inventory. With the initial inventory complete, lake identification was refined, and the lake boundaries were vectorized. The vectors derived from SAR data were validated through field observations carried out on Keller Peninsula in summer and early autumn 2023.

3.2 Determination of backscattering coefficients of lake surfaces in Sentinel-1A imagery

A multitemporal analysis was performed for backscatter and the freeze-thaw dynamics of lake surfaces larger than 1 hectare located on Fildes, Keller and Byers Peninsulas. It is worth noting that for Keller Peninsula only, lakes with surface area smaller than one hectare were analyzed due to the possibility of fieldwork. The minimum area of 1 hectare takes into account the spatial resolution of the images used, following Viel et al. (2022). Thus, 138 Sentinel-1A IW scenes were analyzed, obtained for the months of January, February, March, October, November, and December for the period 2014–2023. This period was chosen because it marks the start of the Sentinel project (2014) and covers spring, summer and early autumn months.

SAR uses electromagnetic waves to detect the presence of objects and determine their position. Unlike solar illumination, which involves continuous parallel radiation of light over a surface, SAR transmits discontinuous pulses of photons from a point source that spread over the terrain as an angular beam (LILLESAND & KIEFER, 1994). The backscattered signal from the target is affected by characteristics of the incident pulse (wavelength, polarization), the radar system geometry relative to the Earth's surface, and the pulse geometry relative to the target (LILLESAND et al., 2008). Several studies have examined ice behavior using radar images, varying in approach, technology, and region. For example, Duguay et al. (2012), Murfitt and Brown (2017) and Zhang and Pavelsky (2019) present different contexts. Jeffries et al. (1994) used C-band SAR images to study lake ice phenology on Alaska's north slope in the winters of 1991 and 1992, identifying backscatter values between −16 dB and −22 dB for frozen surfaces. In comparison, Duguay et al. (2002) employed Radarsat C-band with HH polarization to monitor freeze onset and thaw in subarctic Canadian lakes, validated in the field between November 1997 and May 1998. Surdu et al. (2015) analyzed lake ice phenology in 14 lakes on the Alaskan Coastal Plain using Radarsat-2 C-band (2005–2011), validated with MODIS optical imagery.

Specific backscatter values also vary. Murfitt et al. (2020) reported −21.72 dB for frozen lakes, and Hillebrand et al. (2019) found values below −17 dB for unfrozen surfaces, with values between −14 and −17 dB when up to 60% of the area was frozen. These differences underscore that radar return depends on target geometry and environmental conditions, such as wind. For example, Husman et al. (2021) used Sentinel-1A in VV and VH polarizations for the Athabasca River due to greater sensitivity to wind-roughness compared with HH, which can hinder distinguishing between ice and water (Long et al., 1996). Hillebrand et al. (2019) studied sea ice on the AP using Sentinel-1A in descending orbit, while Malenovsky et al. (2012) argue that both orbits should be considered for monitoring to reduce foreshortening and layover effects in mountainous regions. Da Rosa et al. (2020) found backscatter values higher than −14 dB for frozen lake surfaces.

Backscatter coefficients were obtained via SAR image processing. Images were processed in the SNAP software freely provided by the European Space Agency. That software was developed specifically for processing imagery from Sentinel satellites (ESA, 2024). Images were obtained from the Copernicus platform of the ESA; the product level was GRD (Ground Range Detected) and processing steps included orbit application, calibration, coregistration, conversion of backscatter values to dB and application of the Lee-sigma filter, 5 × 5 window, to remove speckle. Core registration and terrain correction (orthorectification) convert data from terrain geometry to σ° using the DEM. The REMA DEM was used for terrain correction. Additionally, for the temporal analysis of

backscatter values, incidence angle normalization was applied following Eq. (1) (TOPOUZELIS, 2016; ZHOU & ZHENG, 2017; HILLEBRAND et al., 2019). The processing steps for S1-IW images are illustrated in Figure 2. Due to image characteristics and the study area, an incidence angle of 37° was used as a reference (Figure 2).

$$\sigma^{\circ}{}_{ref} = \frac{\sigma^{0}_{\theta} cos^{2}(\theta_{ref})}{cos^{2}(\theta)} \qquad \text{(Equation 01)}$$

Where:
$\sigma^{\circ}{}_{ref}$: Normalized backscatter coefficient;
θ: Local incidence angle;
σ^{0}_{θ}: Measured backscatter coefficient;
θ_{ref}: Reference angle.

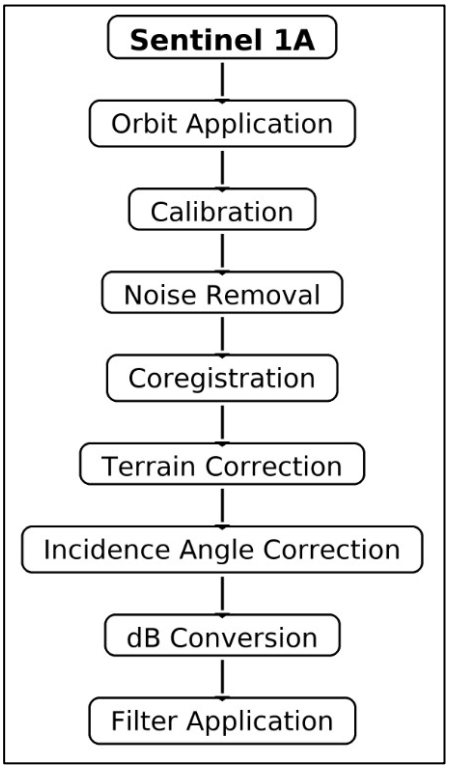

Figure 2. Workflow for processing S1-IW images used to define the backscattering coefficients of the lake surfaces.

3.3 Backscattering and its relationship with climatological variables

Backscatter values were extracted at the automatically generated centroid of each lake vector. The freeze-thaw dynamics of the lakes were related to precipitation (mm), wind direction, wind speed (km/h), mean temperature (°C, daily and monthly), maximum and minimum air temperatures, and the Positive Degree days.

For lake analysis, data from the Presidente Eduardo Frei Montalva meteorological station (62.19194° S, 58.98278° W, altitude 45 m) were used for 1994–2023. This meteorological station is located on Fildes Peninsula and is approximately 32 km from Keller Peninsula and 117 km from Byers Peninsula. Data from a single meteorological station were used for the three peninsulas because, according to Blitz et al. (2018), the mean air temperature series from the Bellingshausen station, located on the same peninsula as Eduardo Frei, can be used to complement and assess the consistency of data series obtained on Livingston Island. The use of atmospheric reanalysis models may be relevant in future studies.

3.4 Statistical analysis of backscatter values

To analyze the distribution of data obtained for each studied lake, the Shapiro-Wilk normality test was used to determine distribution tendencies. According to Razali and Wah (2011), the power of normality tests varies

with significance level and sample size. Statistical analyses were performed using the Google Colab platform, which provides an interactive cloud programming and collaboration environment. Python scripts were used to produce plots related to the temporal analysis. Additionally, the Past software was used for analysis and graphical presentation of temperature, precipitation, wind speed and wind direction means.

3.5 Backscatter and its relationship with slope, hypsometry, and distance from the coastline.

Finally, spatial analysis of slope, hypsometry and distance from the coastline was developed as complementary information to understand lake ice phenology. Geoprocessing techniques were employed for this purpose. Slope was generated in percent using the ArcGIS Slope function. To measure distance to the coastline, the ArcGIS Near function was used, which returns the nearest points between the analyzed vectors, considering a straight line, using lake boundary vectors and the coastline vector as a basis. For hypsometry and slope analysis, the REMA 8 DEM with an 8.8-meter spatial resolution was used. Hypsometry was generated with 20-meter intervals, appropriate for the vertical accuracy of the DEM used. Hypsometry data were distributed into five classes: 0–20 m, 20–40 m, 40–60 m, 60–80 m, and > 80 m. Lake vectors were overlaid onto the hypsometry layer and analyzed according to the class in which they fall. For slope, six amplitude classes were generated: 0–3%; 3–8%; 8–20%; 20–45%; 45–75%; and > 75%. Lake vectors were overlaid onto the slope layer and analyzed by the class they occupy. Figure 3 shows the complete workflow of the study.

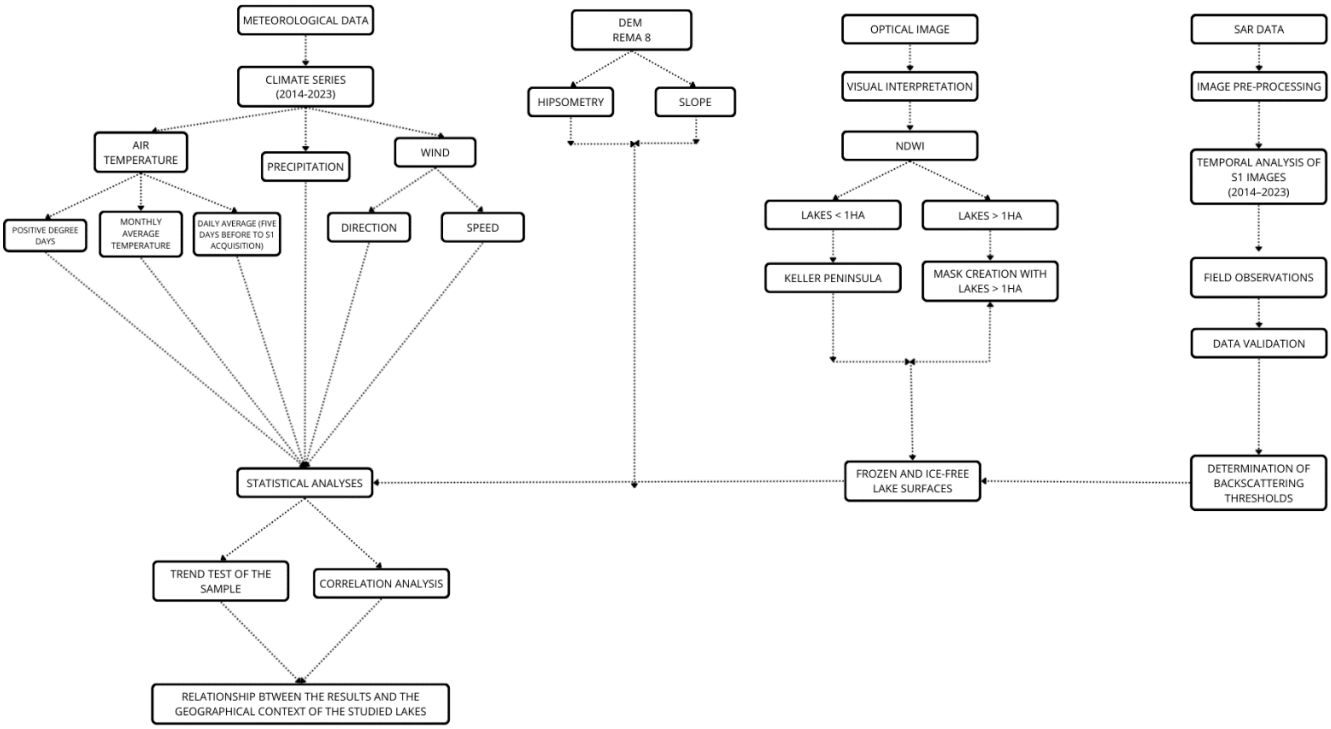

Figure 3. Workflow for obtaining and analyzing lake ice phenology.

4. Results

4.1. Validation analysis for field data and average monthly backscatter values for the period 2014-2023 for the lakes studied in the Fildes, Keller, and Byers peninsulas.

Validation of the adopted threshold considered the work of Da Rosa et al. (2020) and Viel et al. (2022), which indicated that backscatter is a good indicator of changes in lake ice phenology. Viel et al. (2022) demonstrated a visual correspondence between floating ice cover and ice-free areas on the lake surface in S1 images, photographs and TSX imagery when analyzing Fildes Peninsula lakes in February 2015. Following Viel et al. (2022)'s recommendations, field observations were also used for validation on a Keller Peninsula lake for summer 2022/2023 (Table 1). In Figure 4, S1 images obtained on different dates can be observed: the first on 21 February 2023 with the lake surface completely thawed, and the second on 07/10/2023 with the lake surface fully frozen.

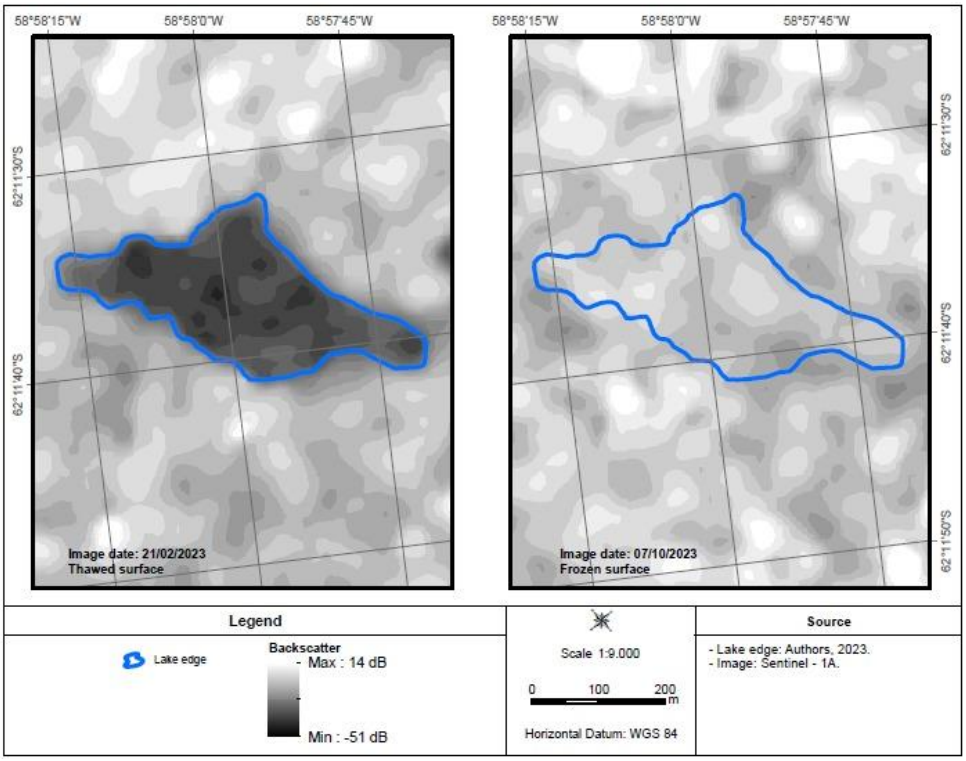

Figure 4. Occurrence of ice-free surface area of lakes located on the Keller Peninsula on 02/21/2023, interpreted from the lower threshold of -15 dB for ice-free water and from field observation.

Table 1 shows four photographs obtained in the field of Keller Peninsula lakes. The four images were obtained on the same days as Sentinel-1A satellite images. In the field photos, the lakes appear completely ice-free. In the radar image, different responses are obtained (< −15 dB for an ice-free lake surface and > −14.9 dB for a frozen lake surface). Most Fildes Peninsula lakes (except lake 11) show higher backscatter values in spring, decreasing toward early summer (December and January) and late summer (February and March). Lakes facing Maxwell Bay exhibited similar behaviors, while lake 11, facing the Drake Passage, displayed a distinct pattern. For Byers Peninsula lakes (except lakes 1, 4 and 7), values are higher in spring and decrease toward early summer (December and January) and late summer (February and March).

Analysis of monthly mean backscatter values for 2014–2023 showed that January predominantly presented backscatter values between −24 dB and −15 dB (Figure 5), with the lowest values obtained in 2023 and the highest in 2016. Similarly, 2015 and 2016 showed higher amplitude in backscatter values while 2020 showed lower amplitude. Regarding the behavior of mean backscatter values for January across the time series, a decrease is observed in 2020 and 2023, and mean values are below −15 dB in all years.

Table 1. Photographs taken during fieldwork on the same dates as the radar images were acquired.

Image date	Photography	Surface condition	Backscatter value (dB)
28/01/2023	Lake surface thawing 	Lake ice-free surfaces	< -15 dB
09/02/2023	Lake surface thawing 	Lake ice-free surface	< -15 dB
21/02/2023	Lake surface thawing 	Lake ice-free surface	< -15 dB
28/04/2023	Lake surface freezing 	Lake frozen surface	> - 14,9 dB

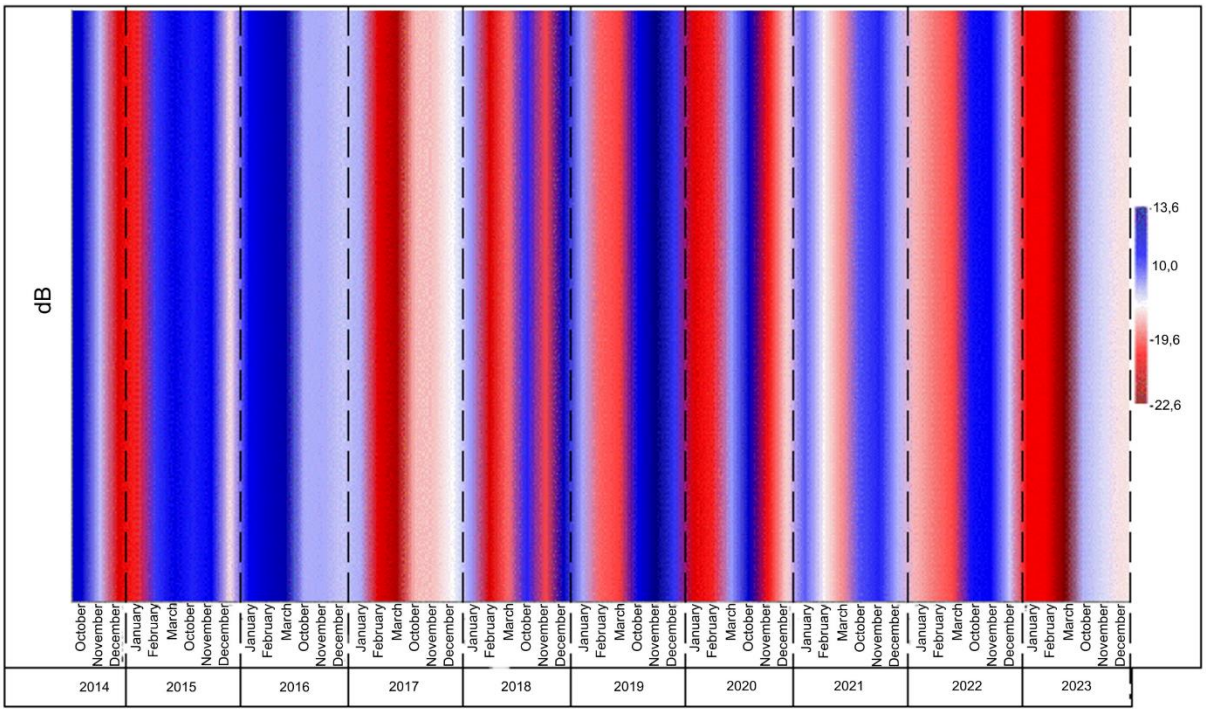

Figure 5. Variation in average backscatter values grouped by month for lakes in the period 2014-2023. Backscatter values below the -15 dB threshold are considered ice-free waters (VIEL et al., 2022). The lowest values were obtained in 2023 and the highest in 2016.

February presented backscatter values between −24 dB and −13 dB, with 2017 showing the largest amplitude. February displayed the highest backscatter values in 2015 and 2016. March exhibited backscatter values between −26 dB and −9 dB (Figure 5), with 2023 showing the lowest values and 2015 and 2016 showing the highest values and amplitudes. For March, a decrease in mean values from 2017 onward is also noted.

For October, backscatter values vary from −21 dB to −9 dB, with 2017 having the lowest values and 2014 the largest amplitude. Mean values increase until 2020, when a decline begins.

November showed backscatter values ranging between −22 dB and −11 dB (Figure 5), with 2015 presenting the lowest values. Note that 2015 and 2014 were the years with the greatest amplitude. The year 2019 showed an atypical behavior for that month, concentrating backscatter values between −15 dB and −12 dB (Figure 5). In December, backscatter values vary from −22 dB to −14 dB (Figure 5), with the largest amplitude in 2022. There is high variability of values in that month across years, except in 2018, which had backscatter values concentrated around −15 dB with little variability.

4.2. Analysis of the climate series and annual backscatter values in the period 2014-2023 for the lakes studied on the Fildes, Keller and Byers peninsulas

Mean air temperature showed an increasing trend ($p = 0.0041$) from 2014 to 2023 (Figure 6). Trend analysis showed no significant trend in minimum temperature ($p = 0.11$); however, maximum temperature exhibited a significant increasing trend ($p = 0.0038$).

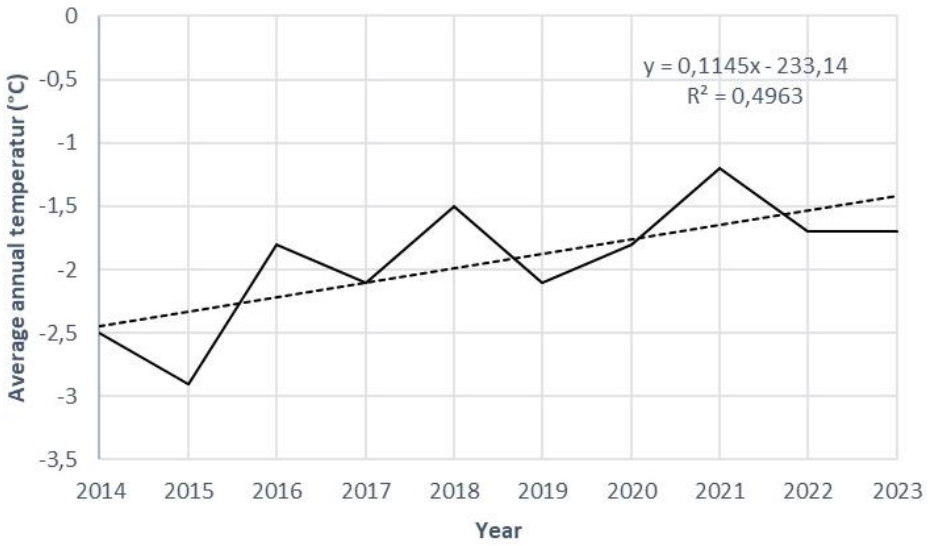

Figure 6. Average air temperature values for the period 2014-2023.

January, February, and March (2014–2023) have higher mean air temperatures, mostly presenting positive temperatures (Figure 7). In general, monthly mean air temperatures for October and November are milder compared to January and February.

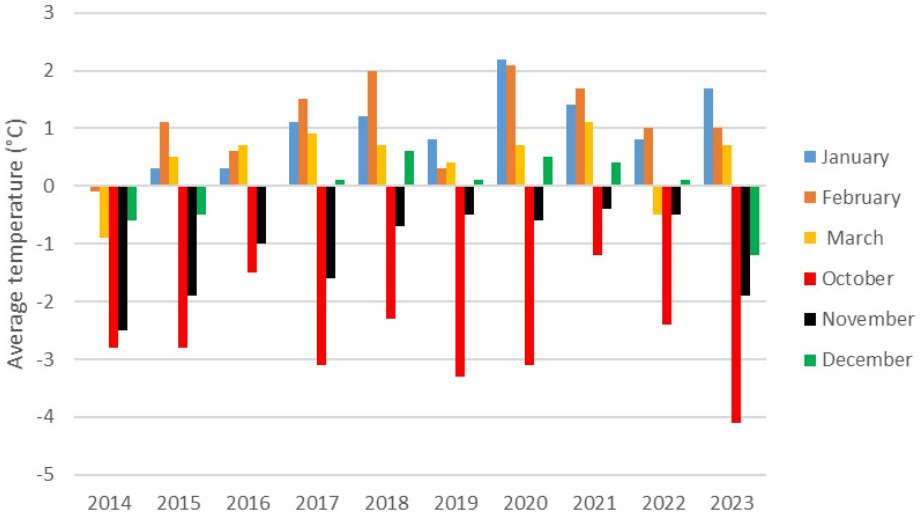

Figure 7. Average air temperature for the months of January, February, March, October, November and December for the period between 2014 and 2023.

From 2018 onward, precipitation decreased, recording the lowest values of the period (Figure 8). It is worth noting that October 2017 had the highest precipitation among months, with measurements above 250 mm. Similarly, a decrease in precipitation was identified for 2021, 2022 and 2023.

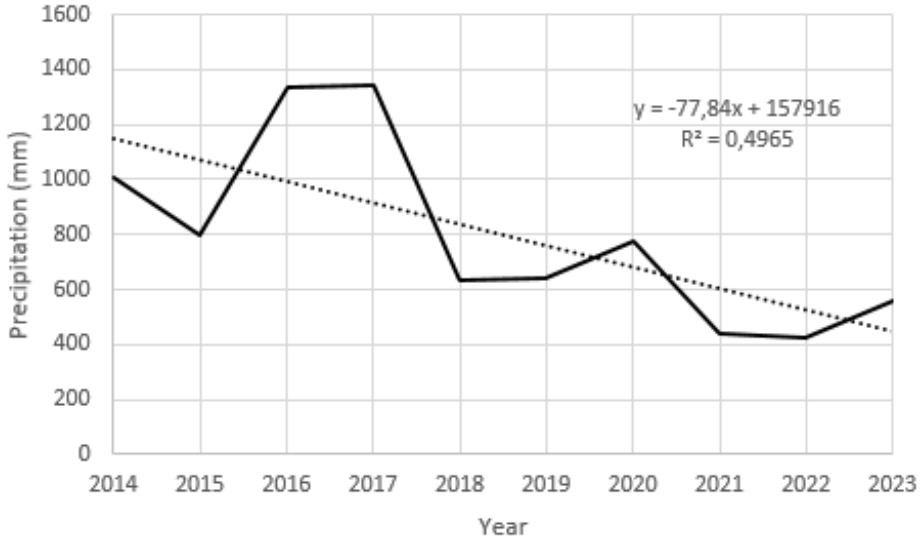

Figure 8. Annual distribution of total precipitation between 2014 and 2023.

Annual mean wind speed has remained constant since 2014, with a slight increase in 2021 and 2022 (Figure 9). Wind direction records show a predominant westward component. Analyzing monthly wind speed distribution for 2014–2023, the wind speed remained practically stable, averaging 17.22 km/h, rarely dropping below 10 km/h.

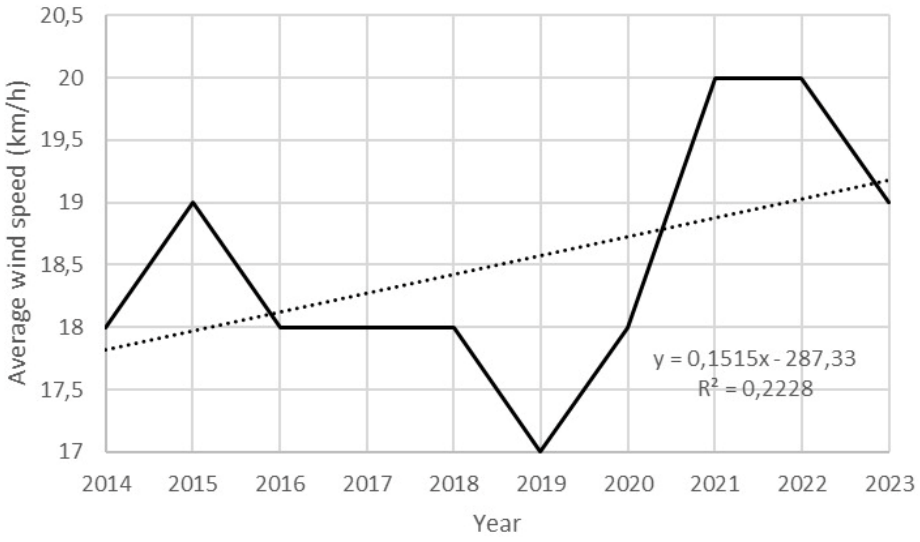

Figure 9. Annual wind speed distribution for the period 2014-2023.

4.3. Relationship between backscatter, wind, mean air temperature and days with positive temperature (STP) in summer for the period 2017–2023

In 2017, lakes analyzed on Fildes and Keller Peninsulas showed higher backscatter values in December, coinciding with reduced wind speed. For January, February, and March 2017, for the three peninsulas studied, backscatter values responded to synoptic conditions, decreasing except on Keller Peninsula, where backscatter values increased with rising air temperature.

In 2018, for Fildes, Keller and Byers Peninsulas, backscatter values increased at the beginning of the series, reflecting a slight drop in mean air temperature. After October, backscatter values decreased, reflecting rising temperature and an increase in days with positive temperatures — a condition that persisted in January, February, and March 2019.

November 2019 shows decreased backscatter values, reflecting rising temperature. From mid-December, there was an increase in mean air temperature, causing backscatter values to decrease for all three peninsulas. Notably, for January, February, and the first 15 days of March 2020, mean air temperature remained positive (Figure 10).

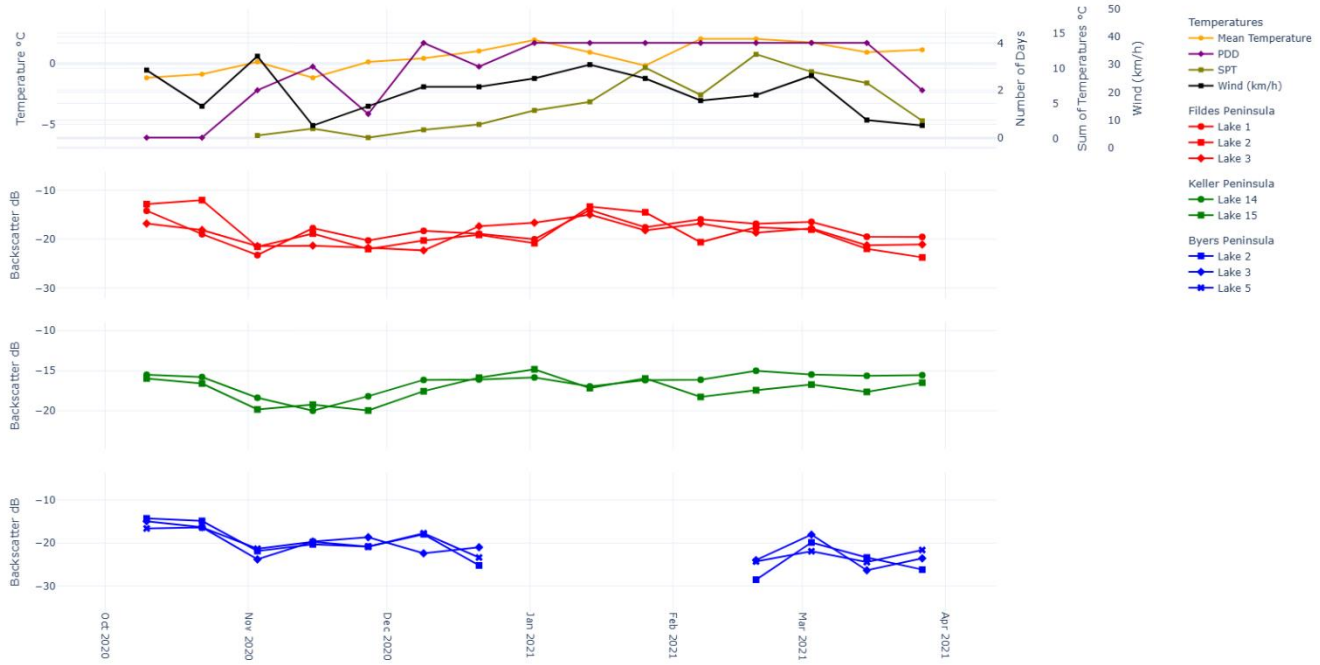

Figure 10. Relationship between backscatter values, mean air temperature, sum of days with positive temperature (PDD) and number of days with positive temperature (SPT) (considering the 5 days before image acquisition) and wind (daily) of the lakes located on the Keller, Byers and Fildes peninsulas. a) characteristics of the months of October, November and December of 2019 and January, February and March of 2020 (period with field data on the Fildes Peninsula).

For October and November 2021, backscatter values decreased, reflecting rising mean air temperature, with a slight increase in backscatter and decrease in mean air temperature in December. Similarly, backscatter values began to decrease at the end of December and remained low until the end of summer 2022, reflecting rising temperature. For October, November, and December 2021, backscatter decreased accompanying the decrease in mean air temperature. From October 2022, backscatter values dropped and remained low until the end of summer 2023, reflecting increased mean air temperature. Field photographs taken in 2023 show lakes completely ice-free and backscatter values corresponding to that class. Values increased only at the start of autumn. For these months, considering the centroid, values ranged between −16.87 dB and −19.34 dB and were low in October, November, and December 2023.

4.5 Hypsometric characteristics, distance from the coast, and slope of the lakes

Lakes 14 and 15 on Keller Peninsula lie at altitudes between 0 and 20 m and are close to the coast; lakes 14 and 15 are 139 m and 138 m from the coast, respectively. Fildes Peninsula lakes 1, 2 and 3 are located between 20 and 40 m altitude; lakes 4, 5, 7 and 10 fall between 40 and 60 m. Finally, lakes 6, 8, 9, 10, 11, 12 and 13 are between 60 and 140 m (Figure 11).

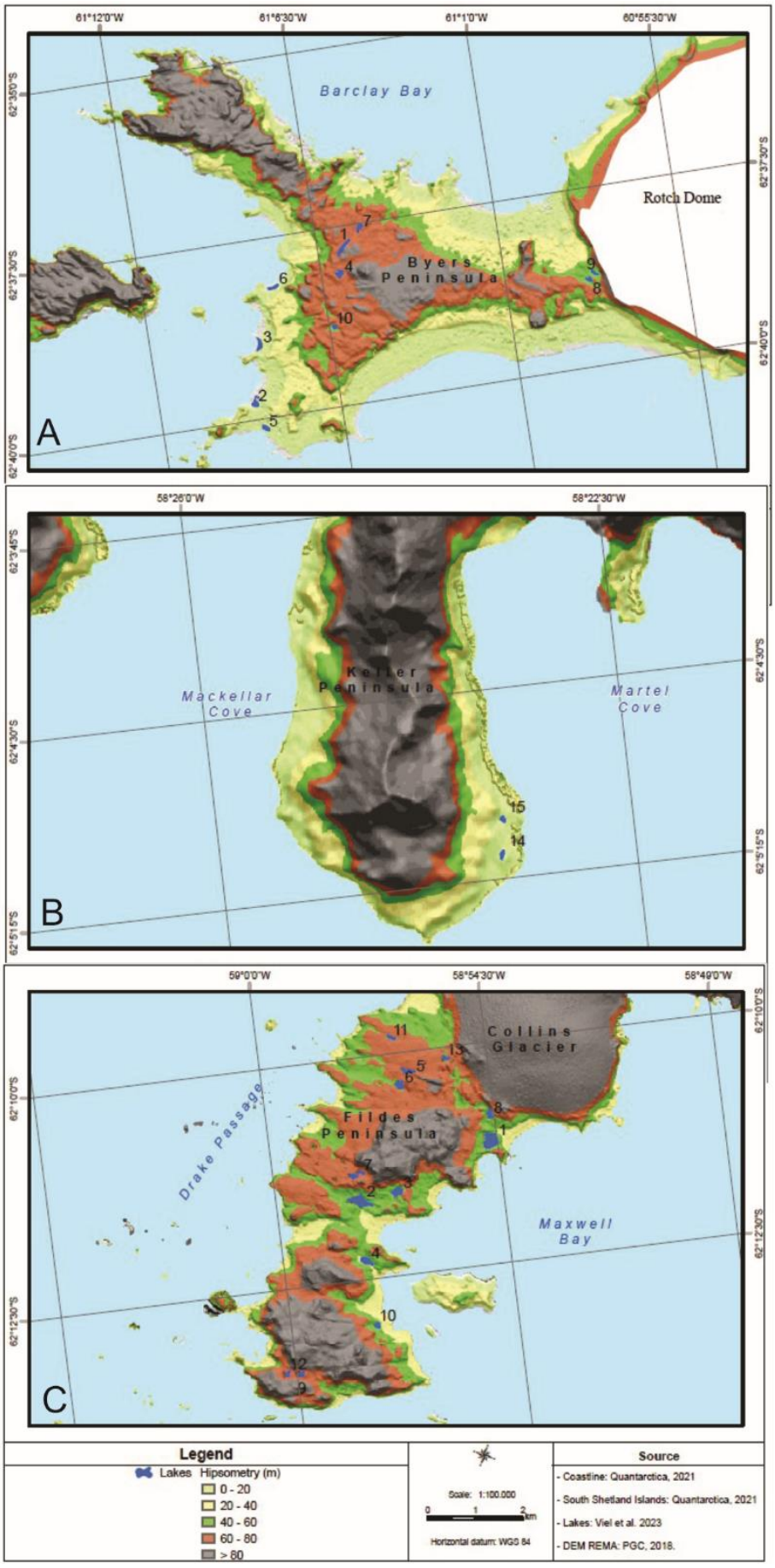

Figure 11. Altitudes of lakes studied on the Fildes, Keller and Byers Peninsulas.

Regarding coastal distance, lake 11 — distinct from the others — is 503 m from the coast and faces the Drake Passage. Lakes 1, 2, 3, 4, 8 and 10 are oriented toward Maxwell Bay. Byers Peninsula lakes are situated at elevations between 0 and 80 m. Lakes 1, 4 and 7 fall in the 60–80 m elevation class and lakes 8, 9 and 10 are in the 40–60 m range. Lakes 2, 3, 5 and 6 are distributed between 0 and 20 m elevation.

When analyzing distance from the coastline relative to the lakes, lakes 1, 4 and 7 are located 1,272 m, 1,200 m and 1,178 m from the coast, respectively (Figure 11). In addition, slope classes where the lakes are located were analyzed and no significant distinctions in their locations were found. Lakes studied on the three peninsulas are found in low slope contexts, located on slopes between 0 and 20%.

5. Discussion

Backscatter values also reflect changes in non-climatic variables such as lake morphometry (depth, area, volume) and elevation (SURDU et al., 2015; LUND et al., 2022). Results show that variation in lake behavior regarding backscatter values and the presence of frozen surface is influenced by geographic factors such as altitude and proximity to the coast, as well as exposure to moist winds, especially for Byers Peninsula lakes. Additionally, among lakes studied on this peninsula, lakes 1, 4 and 7 stand out for having backscatter behaviors different from others. These same lakes are sheltered from wind influence despite differing environmental contexts: lakes 1 and 4 face Osogovo Bay and lake 7 faces Barclay Bay. According to Sobiech and Dierking (2013), in coastal or mountainous environments, wind conditions change locally according to surrounding topography. More specifically, lakes 2, 3, 5 and 6, near the Osogovo Bay coast, are also wind-sheltered; lakes 10 and 11, near Rotch Dome, may be influenced by meltwater and sediment recharge from that dome. Finally, variables such as specific heat capacity cause water temperature to change less proportionally than the environment. Also, larger lakes have greater surface area and are therefore more affected by wind action, which creates waves and facilitates ice breakup.

From this context, distinctions can be explained, among other factors, using hypsometry values where lakes are located. Consequently, coastal or mountainous environments can alter variables such as soil moisture, wind speed and solar exposure, constantly modifying target geometry (SOBIECH & DIERKING, 2013).

Similarly, for Fildes Peninsula lakes, lake 11 stands out with elevated backscatter in the study period and is the only lake facing the Drake Passage with greater wind influence. In contrast, lakes 1, 2, 3, 4, 8 and 10, facing Maxwell Bay, are more sheltered from wind influence. Regarding differences between lakes, lakes 14 and 15 on Keller Peninsula, facing Martel Cove, have similar backscatter values due to a more protected environmental context, differing from less sheltered lakes. Additionally, lake 8 is influenced by proximity to Collins Glacier, unlike others. This factor is related to greater seasonal glacier meltwater input that promotes water movement, mixing of water layers and surface melt, which can result in decreased backscatter values, as noted by Surdu et al. (2015).

In general, a decrease in backscatter values from spring to late summer (December–March) was observed in all lakes, reflecting the thaw cycle from October to April; Surdu et al. (2015) highlight the decline in backscatter with increased lake thaw. This cycle is tied to daily environmental variations, including increased solar radiation, albedo, and mean air temperature. Note that October presented the lowest mean temperatures, predominantly negative, while January–March means were generally positive.

Analyzing annual data, 2015 and 2019 were years with the highest occurrence of lake surface freezing, including freezing periods during summer months. In comparison, from 2020 to 2023 there was a successive increase in mean air temperature, evidencing greater melt during spring.

Regarding spring thaw occurrence, 2017 and 2023 stand out. In 2017 lakes were already ice-free at the beginning of spring, and February and March of that year were also ice-free. Such behavior may relate to a positive SAM (SURYAWANSHI et al., 2023), as well as to anomalies in 2016. Likewise, 2023 is notable for melting in February, March and spring. Backscatter values of the studied lakes reflect, as with sea ice in the region, changes observed in January and February 2023 — a period marked by abrupt Antarctic sea-ice decline (SURYAWANSHI et al., 2023).

Thus, 2015 and 2019 had less thaw, while 2023 set a record with the smallest extent (99.15%) of frozen lake coverage. Mean air temperature appears to be the main factor in lake ice cover variation, with fewer frozen days

in years with more positive temperature occurrences, especially during El Niño events. Finally, climate modes such as SAM and ENSO can alter melt cycle characteristics of lake surfaces (VIEL, 2024).

Moreover, January and February mean backscatter values indicate a general occurrence of lakes with ice-free surfaces, except in January 2023. December is characterized by greater variation in lake surface condition across years, excluding 2018. The year of highest December variability was 2022.

For October, backscatter values show both frozen and ice-free characteristics depending on the year, with 2017 showing the lowest values and 2014 the highest and largest amplitude. Mean values increase until 2020, then decline. This behavior relates to 2019, which for that month exhibited atypical spring and early summer behavior, concentrating backscatter values between −15 dB and −12 dB. Notably, that year showed frozen lakes in December on Fildes Peninsula.

From 2020 onward, the spring change extends into summer: January presented the smallest backscatter amplitude, characterizing an ice-free surface. Analyzing the sum of positive temperatures, January and February 2020 recorded the largest totals. This behavior for 2014–2023 aligns with Turner et al. (2021), who found significant increases in warm days and the record positive temperature on the AP in summer 2020 of 18.4 °C.

A decrease in mean backscatter in March from 2017 onward is noted, accompanying the trend of increasing minimum and mean air temperatures in the region, which favors lake surface melt. Vieira et al. (2024) also recorded this temperature increase at Esperanza Station, with more days above 0 °C. Hass (2023) indicates that intense melts may result from anomalously warm conditions west and east of the AP, roughly 1.5 °C above the mean. A strongly positive SAM influences wind circulation.

Freeze-thaw cycles of the studied lakes are important climatic indicators due to their high-latitude location, as Surdu et al. (2015) emphasize. Studies of ice phenology highlight how these cycles respond directly to air temperature variations, being useful to identify regional climate change (ZHANG & PAVELSKY, 2019).

6. Conclusions

Lake backscatter values are variable and depend on environmental conditions in the days preceding image acquisition. Besides responding to temperature variations, backscatter is also influenced by external environmental factors. The influence of factors such as surrounding moisture, wind speed and lake depth can be evaluated in future studies to deepen analysis and refine interpretation of mechanisms controlling observed responses. Thus, finding a single behavior pattern is difficult; what is observed, even over a short time period, is a trend of increasing mean air temperature reflected in backscatter values and, consequently, in lake phenology.

Results indicate that lake backscatter values respond to air temperature variations. In general, lake thaw begins in October and surfaces freeze again in April. Therefore, the South Shetland Islands are sensitive to small temperature fluctuations, making the lake surface freeze–thaw cycle an important indicator of these regional variations.

Based on identification of the backscatter threshold and its temporal variation, S1 images are applicable to detect and continue monitoring changes in high-latitude lake ice cover. The use of SAR images is also relevant in the Antarctic environment, where field data collection is difficult and frequent cloud cover limits optical sensor use.

Additionally, continuation of studies is recommended to determine and understand backscatter values in autumn and winter, which were not included in this study, since the thaw cycle is better represented in spring and summer. As such, this study represents an initial effort to contribute to monitoring Antarctic lake ice phenology, given the small number of published articles on the topic. Understanding lake phenology at high latitudes also advances other issues such as ecological processes related to ice presence and decomposition and the carbon balance. Therefore, tests using flexible backscatter thresholds for automatic target classification are suggested.

Finally, the lack of meteorological data available for each studied peninsula was a limitation of this work. Moreover, while backscatter can be a good indicator of changes in targets' physical characteristics, it proves limited for quantitative analysis of lake areas. Nevertheless, in-situ data on Keller Peninsula lake phenology, from summer 2023 to early autumn 2023, allowed confirmation of results and comparison with backscatter values obtained from S1 radar images.

Author's contributions: J.A.V.: Conception, Methodology, Research, Writing – initial version, revision and editing. K.K.R.: Conception, Methodology, Research, Supervision, Writing – initial version, revision and editing. C.P.: Methodology, Research, Data Curation, Writing – revision and editing. LF.V.: Methodology, Data Curation, Writing – revision and editing. D.D.A.S.: Research, Writing – revision and editing. F.A.: Research, Writing – revision and editing. R.V.: Methodology, Writing – revision and editing, Visualization.

Acknowledgments: To the Federal University of Rio Grande do Sul and the Postgraduate Program in Geography, as well as to the Federal Institute of Education, Science and Technology of Rio Grande do Sul.

Conflict of Interest: The authors declare no conflict of interest.

References

1. ALFONSO, J. et al. Geochemistry of recent lacustrine sediments from Fildes Peninsula, King George Island, Maritime Antarctica. *Antarctic Science*, v. 27, n. 5, p. 462–471, 2015.
2. ANDRADE, A. M. Variabilidade na camada ativa do solo na Meseta Norte e na superfície da Península Fildes, Ilha Rei George, Antártica Marítima. 2017. Tese (Doutorado em Geografia) – Programa de Pós-Graduação em Geografia da Universidade Federal do Rio Grande do Sul, Porto Alegre, 2017.
3. BLITZ, R.; NAVARRO, F. J.; OTERO, J. LAPAZARAN, J.; GONZALEZ, S. Effects of recent cooling in the Antarctic Peninsula on snow density and surface mass balance. *Polish Polar Research*, v. 39, p. 457–480, 2018.
4. C3S. Copernicus Climate Change Service. 2020 warmest year on record for Europe; globally, 2020 ties with 2016 for warmest year recorded, 2021.
5. CARRIVICK, J.; HECKMANN, T. Short-term geomorphological evolution of proglacial systems. *Geomorphology*, v. 287, p. 1–13, 2017.
6. CURL, J. E. A glacial history of the South Shetland Islands, Antarctica. Columbus: Ohio State University, 1980. p. 146.
7. DA ROSA, N. C.; BREMER, U. F.; FILHO, W. P.; SOUSA JÚNIOR, M. A.; KRAMER, G.; HILLEBRAND, L. F.; JESUS, J. B. DE. Freezing and thawing of lakes on the Nelson and King George Islands, Antarctic, using Sentinel 1A synthetic aperture radar images. *Environ Monit Assess*, v. 192, 559, 2020. DOI: /10.1007/s10661-020-08526-5.
8. DIRSCHERL, M.; DIETZ, A. J.; KNEISEL, C.; KUENZER, C. A. Novel method for automated supraglacial lake mapping in Antarctica using Sentinel-1 SAR imagery and deep learning. *Remote Sensing*, v. 13, 197, 2021. DOI: /10.3390/rs13020197.
9. DUGUAY, C.; BROWN, L.; KANG, K.-K.; KHEYROLLAH POUR, H. The Arctic lake ice, in "State of the Climate in 2011". *Bulletin of the American Meteorological Society*, v. 93, p. S152-S154, 2012.
10. ESA. The European Space Agency. TerraSAR-X ESA archive. 22 abr. 2022. Disponível em: https://earth.esa.int/eogateway/catalog/terrasar-x-esa-archive. Acesso em: 24 set. 2022.
11. ESA. The European Space Agency. Imagens Sentinel. Disponível em: https://browser.dataspace.copernicus.eu/. Acesso em: 20 dez. 2023.
12. ESA. The European Space Agency. Sentinel Application Platform (SNAP) – ESA Sentinel Scientific Toolbox: version 9.0.0. Disponível em: https://step.esa.int/main/download/snap-download/. Acesso em: 6 nov. 2025.
13. FARIA, A. L. L. DE. Solos, geomorfologia e relações ecológicas na parte sudoeste da Península de Byers, Ilha Livingston, Antártica Marítima. 2010. Tese (Doutorado) – Universidade Federal de Viçosa, Viçosa, 2010.
14. FRANCELINO, M.R. Geoformas da Península Keller, Antártica Marítima: subsídios ao monitoramento ambiental. In: SCHAEFER, C.E.G.R.(Ed.); FRANCELINO, M.R; SIMAS, F.N; ALBUQUERQUE FILHO, M.R. Ecossistemas costeiros e monitoramento ambiental da Antártica Marítima, Viçosa, NEPUT, 2004. p.15- 25.
15. GALVÃO, J. C. de M., et al. Analysis of shallow lake sediments in the Fildes Peninsula, King George Island, Maritime Antarctica. *Revista Brasileira de Geomorfologia*, 21, p. 217 - 234, 2020. DOI: 10.20502/rbg.v21i2.1738.
16. HILLEBRAND, L. F.; DA ROSA, C. N.; COSTI, J.; BREMER, U. F. Mapeamento do gelo marinho na Península Antártica com imagens Sentinel-1A. *Anuário do Instituto de Geociências*, v. 42, p. 59-71, 2019. DOI: http://dx.doi.org/10.11137/2019_2_59_71.
17. IVANOV, L. L. Antarctica: Livingston Island and Greenwich, Robert, Snow and Smith Islands. Scale 1:120000 topographic map. Troyan: Manfred Wörner Foundation, 2010.
18. JEFFRIES, M. O.; MORRIS, K.; WEEKS, W. F.; WAKABAYASHI, H. Structural and stratigraphic features and ERS-1 synthetic aperture radar backscatter characteristics of ice growing on shallow lakes in NW Alaska, winter 1991-1992. Journal of Geophysical Research, v. 99, p. 22459-22471, 1994. DOI: http://dx.doi.org/10.1029/94jc01479.

19. JONES, J. M. Assessing recent trends in high-latitude southern hemisphere surface climate. *Nature Climate Change*, v. 6, p. 917–926, 2016.
20. MENDES JUNIOR, C. W.; DANI, N.; ARIGONY-NETO, J.; SIMÕES, J. C.; BREMER, U. F.; JÚNIOR, E. S. F.; ERWES, H. J. B. Análise morfométrica da Península Keller, Antártica, através do SIG. *Revista Brasileira de Cartografia*, n. 62/04, p. 1–12, 2010.
21. KROPÁČEK, J.; MAUSSION, F.; CHEN, F.; HOERZ, S.; HOCHSCHILD, V. Analysis of ice phenology of lakes on the Tibetan Plateau from MODIS data. *Cryosphere*, v. 7, p. 287–301, 2013. DOI: 10.5194/tc-7-287-2013.
22. LILLESAND, T. E.; KIEFER, R. W; CHIPMAN, J.W. Remote Sensing and Image Interpretation. *New York: John Wiley & Sons*, 7ª ed., 750 p., 2008.
23. LONG, D. G.; COLLYER, R. S.; ARNOLD, D. V. Dependence of the normalized radar cross section of water waves on Bragg wavelength–wind speed sensitivity. *IEEE Transactions on Geoscience and Remote Sensing*, v. 34, p. 656–666, 1996. DOI: 10.1109/36.499745.
24. LUND, J.; FORSTER, R.; DEEB, E. J.; LISTON, G. E.; SKILES, M.; MARSHALL, H. P. Interpreting Sentinel-1 SAR Backscatter Signals of Snowpack Surface Melt/Freeze, Warming, and Ripening, through Field Measurements and Physically-Based SnowModel. *Remote Sensing*, v. 14, p. 1 - 28, 2022. DOI: 10.3390/rs14164002.
25. MATSUOKA, K.; SKOGLUND, A.; ROTH, G.; POMEREU, J.; GRIFFITHS, H.; HEADLAND, R.; HERRIED, B.; KATSUMATA, K.; BROCQ, A. L.; LICHT, K.; MORGAN, F.; NEFF, P. D.; RITZ, C.; SCHEINERTL, M.; TAMURA, T.; PUTTE, A. V. de; BROEKE; M. V. de; DESCHWANDEN, A. V.; DESCHAMPS-BERGER, C.; LIEFFERINGE, B. V.; TRONSTAD, S.; MELVÆR, Y. Quantarctica, an integrated mapping environment for Antarctica, the Southern Ocean, and sub-Antarctic islands. *Environmental Modelling and Software*, v. 140, p. 1- 14, 2021. DOI: 10.21334/NPOLAR.2018.8516E961.
26. MARSHALL, S. J. Regime shifts in glacier and ice sheet response to climate change: examples from the Northern Hemisphere. *Frontiers in Climate*, v. 3, 2021.
27. MURFITT, J.; BROWN, L. C. Lake ice and temperature trends for Ontario and Manitoba: 2001 to 2014. *Hydrological Processes*, v. 31, p. 3596-3609, 2017. DOI: 10.1002/hyp.11295.
28. MURFITT, J.; DUGUAY, C. R. Assessing the performance of methods for monitoring ice phenology of the world's largest high Arctic lake using high-density time series analysis of Sentinel-1 data. *Remote Sensing*, v. 12, p. 1-25, 2020. DOI: 10.3390/rs12030382.
29. O'REILLY, C. M. Rapid and highly variable warming of lake surface waters around the globe. *Geophysical Research Letters*, v. 42, p. 1-9, 2015. DOI: 10.1002/2015GL066235.
30. PABLO, M. A. de. Timelapse images datasets (2017–2022) from Livingston and Deception Islands, Antarctica, to study snow cover and weather conditions at the PERMATHERMAL monitoring network. Data in Brief, v. 52, p. 1 - 14, 2024. DOI: /10.1016/j.dib.2023.109970.
31. PETSCH, C.; ROSA, K. K. DA.; OLIVEIRA, M. A. DE.; VELHO, L. F.; SILVA, S. L. C. S.; SOTILLE, M. E.; VIEIRA, R.; SIMÕES, J. C. An inventory of glacial lakes in the South Shetland Islands (Antarctica): temporal variation and environmental patterns. *Anais da Academia Brasileira de Ciência*s, p. 1–26, 2022.
32. PETSCH, C.; COSTA, R. M.; SIMÕES, J. C.; SOTILLE, M. E.; ROSA, K. K. DA. Cambios climáticos y aumento de la vegetación en la Península Fildes, Antártica. *Investigaciones Geográfica*s, v. 57, p. 18-31, 2018. DOI: 10.5354/0719-5370.2019.52147.
33. PETSCH, C.; COSTA, R. M.; ROSA, K. K. DA.; VIEIRA, R.; BRAUN, M. H.; SIMÕES, J. C. Desenvolvimento hidrológico e fenologia de lagos da Península Fildes – *Antártica. Geociência*s, v. 39, n. 2, p. 145–162, 2020. DOI: 10.5016/gv39i2.14453.
34. RAZALI, N. M.; WAH, Y. B. Power comparisons of Shapiro-Wilk, Kolmogorov-Smirnov, Lilliefors and Anderson-Darling tests. *Journal of Statistical Modeling and Analytic*s, v. 2, n. 1, p. 21-33, 2011.
35. ROSA, C. N.; BREMER, U. F.; FILHO, W. P.; JUNIOR, M. A. S.; KRAMER, G.; HILLEBRAND, F. L.; JESUS, J. B. Freezing and thawing of lakes on the Nelson and King George Islands, Antarctica, using Sentinel-1A synthetic aperture radar images. *Environmental Monitoring and Assessmen*t, v. 192, p. 559, 2020.
36. SHUGAR, D. H.; BURR, A.; HARITASHYA, U. K.; KARGEL, J. S.; WATSON, S. C.; KENNEDY, M. C.; BEVINGTON, A. R.; BETTS, R. A.; HARRISON, S.; STRATTMAN, K. Rapid worldwide growth of glacial lakes since 1990. *Nature Climate Change*, v. 10, P. 939–945, 2020.
37. SURDU, C. M.; DUGUAY, C. R.; POUR, H. K.; BROWN, L. C. Ice freeze-up and break-up detection of shallow lakes in Northern Alaska with spaceborne SAR. *Remote Sens*. 7, 6133–6159. 2015.
38. SURYAWANSHI, K.; JENA, B.; BAJISH, C. C.; ANILKUMAR, N. Recent Decline in Antarctic Sea Ice Cover From 2016 to 2022: Insights From Satellite Observations, Argo Floats, and Model Reanalysis. *Tellus A: Dynamic Meteorology and Oceanography*, 75, p. 193 – 212, 2023. DOI:/10.16993/tellusa.3222.

39. SIMÕES, J.C.; DANI, N.; BREMER, U. F.; AQUINO, F. E.; ARIGONY-NETO, J. Small cirque glaciers retreat on Keller Peninsula, Admiralty Bay, King George Island, Antarctica. *Pesquisa Antártica Brasileira*, v.4, p.49-56, 2004.
40. ŠMEJKALOVÁ, T.; EDWARDS, M. E.; DASH, J. Arctic lakes show strong decadal trend in earlier spring ice-out. *Scientific Reports*, v. 6, p. 1-8, 2016. DOI: 10.1038/srep38449.
41. SOBIECH, J.; DIERKING, W. Observing lake- and river-ice decay with SAR: Advantages and limitations of the unsupervised k-means classification approach. *Annals of Glaciology*, v. 54, p. 65-72, 2013. DOI: 10.3189/2013AoG62A037.
42. SURDU, C. M.; DUGUAY, C. R.; POUR, H. K.; BROWN, L. C. Ice freeze-up and break-up detection of shallow lakes in northern Alaska with space-borne SAR. *Remote Sensing*, v. 7, p. 6133-6156, 2015. DOI: 10.3390/rs70506133.
43. TOPOUZELIS, K.; SINGHA, S.; KITSIOU, D. Incidence angle normalization of wide swath SAR data for oceanographic applications. *Open Geosciences*, v. 8, p. 450–464, 2016. Disponível em: https://doi.org/10.1515/geo-2016-0029. Acesso em: 23 jul. 2024.
44. TURNER, J. Extreme temperatures in the Antarctic. *Journal of Climate*, v. 34, p. 2653–2668, 2021.
45. TURNER, J. The SCAR READER project: toward a high-quality database of mean Antarctic meteorological observations. *Journal of Climate*, v. 17, p. 2890–2898, 2004.
46. VAUGHAN, D. G. Recent rapid regional climate warming on the Antarctic Peninsula. *Climate Change*, v. 60, p. 243–274, 2003.
47. VIEIRA, R.; CARDOSO, P.; ROSA, K. K. DA.; PETSCH, C.; LIRIO, J. M. Changes and collapse in lacustrine system in Antarctic Peninsula ice-free area: Boeckella and Buenos Aires lakes. *Anais da Academia Brasileira de Ciências*, v.96, n.2, 2024. DOI: 10.1590/0001-3765202420240578
48. VIEIRA, R.; ROSA, K. K. DA.; SIMÕES, C. L.; FERREIRA, F.; SANTOS, J. V.; GONÇALVES, M.; RODRIGUES, R. I.; FELIZARDO, J. P. Análisis sedimentológico y geomorfológico de áreas lacustres en la Península Fildes, Isla Rey Jorge, Antártica Marítima. *Investigaciones Geográficas*, v. 0, p. 3–30, 2015.
49. VIEL, J. A. Fenologia do gelo de lagos nas penínsulas Byers, Keller e Fildes, Antártica Marítima, no período de 2014 a 2023 com dados SAR. Tese (Doutorado). Universidade Federal do Rio Grande do Sul. Instituto de Geociências. Programa de Pós-Graduação em Geografia. 2024. 131p.
50. VIEL, J. A.; PETSCH, C.; VELHO, L. F.; ROSA, K. K. Lake ice phenology: a comparison between TSX and Sentinel-1 images using field data analysis in a maritime Antarctica region. Investigaciones Geográficas, n. 63, p. 89–103, 2022.
51. WATCHAM, E. P.; BENTLEY, M. J.; HODGSON, D. A.; ROBERTS, S. J.; FRETWELL, P. T.; LLOYD, J. M.; LARTER, R. D.; WHTEHOUSE, P. L.; LENG, M. J.; MONIEN, P.; MORETON, S. G. A new Holocene relative sea level curve for the South Shetland Islands, *Antarctica. Quaternary Science Reviews*, v. 30, p. 3152–3170, 2011. Disponível em: https://doi.org/10.1016/j.quascirev.2011.07.021. Acesso em: 23 jul. 2024.
52. WOOLWAY, R. I.; KRAEMER, B. M.; LENTERS, J. D.; MERCHANT, C. J.; O'REILLY, C. M.; SHARMA, S. Global lake responses to climate change. *Nature Reviews Earth & Environment*, v. 1, p. 388–403, 2020.
53. ZHANG, S.; PAVELSKY, T. M. Remote sensing of lake ice phenology across a range of lake sizes, ME, USA. *Remote Sensing*, v. 11, p. 1–13, 2019. Disponível em: https://doi.org/10.3390/rs11141718. Acesso em: 23 jul. 2024.
54. ZHOU, C.; ZHENG, L. Mapping radar glacier zones and dry snow line in the Antarctic Peninsula using Sentinel-1 images. *Remote Sensing*, v. 9, p. 1171, 2017.